

Numerical estimation of dynamic transmission error of gear by using quasi-flexible-body modeling method[†]

Sunggyu Cho¹, Juhwan Choi¹, Jin Hwan Choi² and Sungsoo Rhim^{2,*}

¹FunctionBay, Inc., 5F, Pangyo Seven Venture Valley 1 danji 2 dong, 15, Pangyo-ro 228 beon-gil, Bundang, Seongnam, Gyeonggi, 463-400, Korea

²Kyunghee University, Yongin, Gyeonggi, 449-791, Korea

(Manuscript Received December 29, 2014; Revised April 2, 2015; Accepted April 24, 2015)

Abstract

When the power transmission systems are designed or improved, an understanding of gear dynamics is essential and very important. Gear systems are not easy to investigate because gear noise has to be carefully controlled. As a result, when designing and developing gear transmission systems, it is very important to grasp the noise and reduce it. Also, it is necessary to make a clear distinction between rattle noises and whine noises. The rattle noise occurs by mainly hitting the tooth, and whine noise occurs by mainly rubbing the tooth in meshing. Therefore, the whine noise is relatively related to high frequency characteristics. Our aim was to find a good way to evaluate whine noise with a numerical approach. When the gear dynamics are investigated to evaluate the whine noise, the dynamic transmission error (DTE) can be utilized. But, it is very difficult to obtain the DTE results by means of not only experimental ways but also numerical calculations. Although multi-body dynamics software has not been able to calculate the DTE practically yet, there is a possibility that the software can get the DTE results. Therefore, we propose a numerical modeling method to obtain the DTE results by using multi-body dynamics software (RecurDyn). To reduce the calculation time and represent flexibility, a rotational joint and force element with the bending stiffness are applied between gear teeth and trunk. Also the numerical results have been compared with the experimental data. The results show a good agreement with the experimental results.

Keywords: Dynamic transmission error (DTE); Gear noise; Multi-body dynamics (MBD); Quasi-flexible-body (QFB) gear

1. Introduction

To precisely estimate and obtain the dynamic transmission error (DTE), an efficient numerical model should be defined carefully to simulate the phenomena of high frequency characteristics. We have adopted a numerical model with a bending stiffness between a gear tooth and a gear trunk. To equivalently represent the flexibility with a bending stiffness, we propose a flexible model having a rotational joint with a bending stiffness for joining the gear tooth and trunk so as to reduce the calculation time and to make a simple and easy model, which we call the Quasi-flexible-body (QFB) gear model. The proposed QFB gear model is shown in Fig. 1. In the QFB gear model, rotational joints and force elements with bending stiffness are generated between teeth and trunk in order to consider the flexibility of gear teeth. As a result, teeth can be rotated by the applied gear contact forces. If a contact force is generated between gears, this contact force will be applied on the gear tooth and

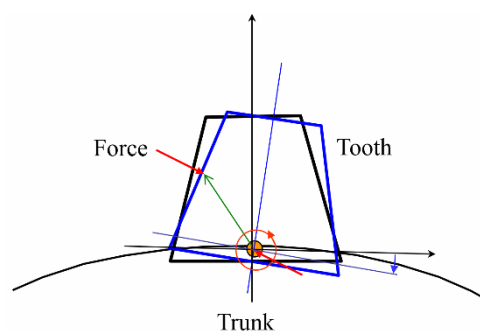


Fig. 1. Quasi-flexible-body gear model.

this force will rotate the gear tooth as shown in Fig. 1. To represent the vibration phenomena of the gear tooth, the generalized force and torque acting on the gear tooth are calculated from the gear contact force which is generated by a gear tooth contact algorithm. For the gear contact, this paper uses an involute curve which is approximated with several arc segments. To verify the proposed method, the numerical results have been compared with a reliable experimental data [1] for the DTE. The proposed numerical model shows a good agreement with the experimental data.

*Corresponding author. Tel.: +82 31 201 3248, Fax.: +82 31 202 8106
E-mail address: ssrhim@khu.ac.kr

[†]This paper was presented at the Joint Conference of the 3rd IMSD and the 7th ACMD, Busan, Korea, June, 2014. Recommended by Guest Editor Sung-Soo Kim and Jin Hwan Choi

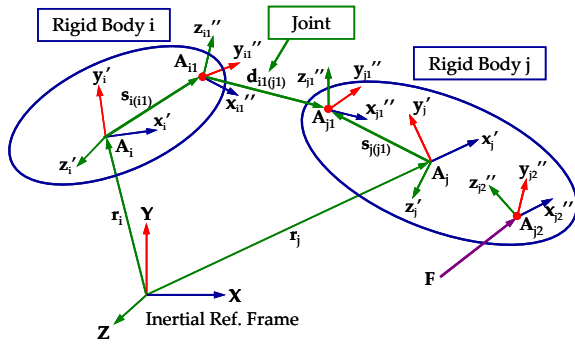


Fig. 2. Two contiguous rigid bodies.

2. Multi-body dynamics (MBD) formulation

Rigid body dynamics can be modeled using various formulations [2]. In this investigation, the recursive formulation is used. This section provides a brief introduction to the recursive formulation. The coordinate systems for two contiguous rigid bodies in 3D space are shown in Fig. 2. Two rigid bodies are connected by a joint, and an external force F is acting on the rigid body j . X - Y - Z is the inertial or global reference frame and x' - y' - z' is the body reference frame with respect to the X - Y - Z frame. The subscript i means the inboard body of the body j in the spanning tree of the recursive formulation [3, 4].

Velocities and virtual displacements of the origin of the body reference frame x' - y' - z' with respect to the global reference frame X - Y - Z , respectively, can be defined as follows:

$$\begin{bmatrix} \dot{\mathbf{r}} \\ \boldsymbol{\omega} \end{bmatrix}, \tag{1}$$

and

$$\begin{bmatrix} \delta \mathbf{r} \\ \delta \boldsymbol{\pi} \end{bmatrix}. \tag{2}$$

Their corresponding quantities with respect to the body reference frame x' - y' - z' are, respectively, defined as follows:

$$\mathbf{Y} = \begin{bmatrix} \dot{\mathbf{r}}' \\ \boldsymbol{\omega}' \end{bmatrix} \equiv \begin{bmatrix} \mathbf{A}^T \dot{\mathbf{r}} \\ \mathbf{A}^T \boldsymbol{\omega} \end{bmatrix}, \tag{3}$$

and

$$\delta \mathbf{Z} = \begin{bmatrix} \delta \mathbf{r}' \\ \delta \boldsymbol{\pi}' \end{bmatrix} \equiv \begin{bmatrix} \mathbf{A}^T \delta \mathbf{r} \\ \mathbf{A}^T \delta \boldsymbol{\pi} \end{bmatrix}, \tag{4}$$

where \mathbf{A} is the orientation matrix of the x' - y' - z' frame with respect to the X - Y - Z frame. The recursive velocity equations for a pair of contiguous bodies and the recursive virtual displacement relationships are, respectively,

$$\mathbf{Y}_j = \mathbf{B}_{ij}^1 \mathbf{Y}_i + \mathbf{B}_{ij}^2 \dot{\mathbf{q}}_{ij}, \quad \delta \mathbf{Z}_j = \mathbf{B}_{ij}^1 \delta \mathbf{Z}_i + \mathbf{B}_{ij}^2 \delta \mathbf{q}_{ij}, \tag{5}$$

where \mathbf{Y}_j is the combined vector of Cartesian translational and rotational velocities relative to the body reference frame j , as defined in Eqs. (3) and (4), \mathbf{q}_{ij} is the vector of joint coordinates for the joint connecting body i and j , $\dot{\mathbf{q}}_{ij}$ is the time derivative of \mathbf{q}_{ij} , \mathbf{B}_{ij}^1 is the velocity transformation matrix that relates Cartesian velocities in the body reference frame i to the body reference frame j , and \mathbf{B}_{ij}^2 is the velocity transformation matrix that relates joint velocities of the joint between bodies i and j to Cartesian velocities in the body reference frame j . Recursively applying Eq. (5) to all joints along the spanning tree, the following relationship between the Cartesian and relative generalized velocities can be obtained as follows:

$$\mathbf{Y} = \mathbf{B} \dot{\mathbf{q}}, \tag{6}$$

where \mathbf{B} is the collection of the coefficients of $\dot{\mathbf{q}}_{ij}$ and

$$\mathbf{Y} = \left[\mathbf{Y}_0^T, \mathbf{Y}_1^T, \mathbf{Y}_2^T, \dots, \mathbf{Y}_n^T \right]_{nc}^T, \tag{7}$$

$$\dot{\mathbf{q}} = \left[\dot{\mathbf{q}}_0^T, \dot{\mathbf{q}}_{01}^T, \dot{\mathbf{q}}_{12}^T, \dots, \dot{\mathbf{q}}_{(n-1)n}^T \right]_{nr}^T, \tag{8}$$

where nc and nr denote the number of the Cartesian and relative generalized coordinates, respectively. The Cartesian velocity $\mathbf{Y} \in \mathbf{R}^{nc}$ with a given $\dot{\mathbf{q}} \in \mathbf{R}^{nr}$ can be evaluated either by using Eq. (6) obtained from symbolic substitutions or by using Eq. (5) with recursive numerical substitution of \mathbf{Y}_j .

It is often necessary to transform a vector \mathbf{G} , which is a vector in \mathbf{R}^{nc} , into a new vector $\mathbf{g} = \mathbf{B}^T \mathbf{G}$ in \mathbf{R}^{nr} . Such a transformation can be found from the generalized force computation in the joint space with a known force in the Cartesian space. The virtual work done by a Cartesian force $\mathbf{Q} \in \mathbf{R}^{nc}$ is obtained as follows:

$$\delta \mathbf{W} = \delta \mathbf{Z}^T \mathbf{Q}, \tag{9}$$

where $\delta \mathbf{Z}$ must be kinematically admissible for all joints in a system. Substitution of $\delta \mathbf{Z} = \mathbf{B} \delta \mathbf{q}$ into Eq. (9) yields

$$\delta \mathbf{W} = \delta \mathbf{q}^T \mathbf{B}^T \mathbf{Q} = \delta \mathbf{q}^T \mathbf{Q}^*, \tag{10}$$

where $\mathbf{Q}^* \equiv \mathbf{B}^T \mathbf{Q}$.

The equation of motion for a constrained mechanical system in the joint space is then obtained by using the velocity transformation method as follows [5, 6]:

$$\mathbf{F} = \mathbf{B}^T (\mathbf{M} \dot{\mathbf{Y}} + \boldsymbol{\Phi}_Z^T \boldsymbol{\lambda} - \mathbf{Q}) = \mathbf{0}, \tag{11}$$

where $\boldsymbol{\Phi}$ and $\boldsymbol{\lambda}$, respectively, denote the cut joint constraint and the corresponding Lagrange multiplier. \mathbf{M} is the mass

Table 1. Two QFB gear types.

	Joint type	Force type
Case1	Spherical	3D rotational spring
Case2	Revolute	1D rotational spring

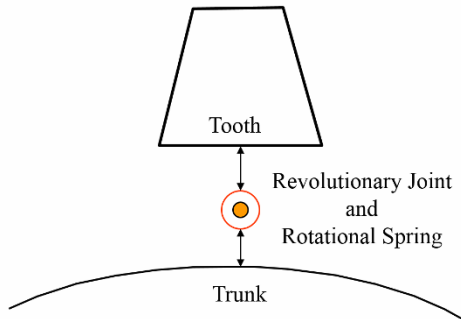


Fig. 3. Basic concept of QFB gear.

matrix and Q is the force vector including the external forces in the Cartesian space.

3. Modeling methods

3.1 Quasi-flexible-body gear model

In general, a finite element method (FEM) is widely used to represent the flexibility. But the FEM takes much calculation time because of having many “Degrees of freedom.” Therefore, to overcome this situation, we have adopted a new, efficient modeling method called Quasi-flexible-body (QFB). To equivalently represent the flexibility with the bending stiffness, the QFB gear model has a rotational joint with a bending stiffness for joining the gear tooth and trunk of rigid body, so as to reduce the calculation time and to make a simple and easy numerical model. The basic concept of the QFB gear is shown in Fig. 3.

There are two connection types for QFB gear to consider the flexibility of the gear teeth. The connection types for joints and forces are summarized in Table 1.

A schematic diagram for the QFB gear model is shown in Fig. 4.

In Fig. 4, θ is the angular displacement of gear, ϕ is the angular displacement of the tooth, r_g is the position vector of the center of gravity (COG) of gear, r_j is the position vector for joint point from the gear center, r_{gt} is the position vector for the COG of the tooth from the joint point, r_{gt-o} is the position vector of the COG of the tooth from the inertial reference frame, r_c is the position vector for the contact point from the joint point. r_{gt} and r_{gt-o} can be changed when the external forces act on the tooth. This is a major difference of QFB gear as compared with a rigid gear.

M_g is the mass of gear, M_{gt} is the mass of tooth, I_g is the moment of inertia of gear, I_{gt} is the moment of inertia of tooth, F_{gs} is the force vector acting on the gear shaft, T_{gs} is the torque acting on the gear shaft, F_j is the force vector

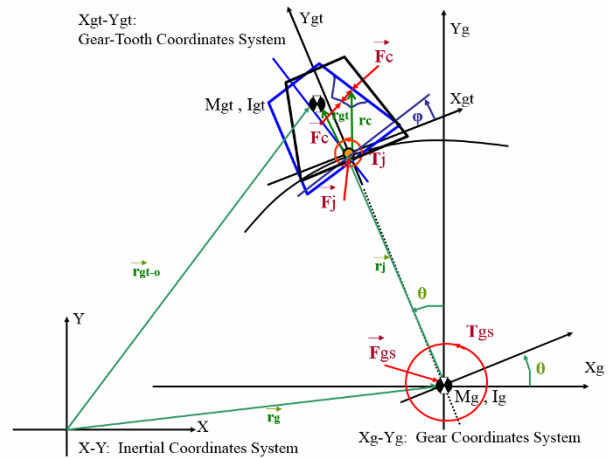


Fig. 4. Schematic diagram for QFB gear model.

acting on the tooth at the joint, T_j is the torque acting on the tooth at the joint, and F_c is the force vector acting on the gear contact area.

3.2 Contact force model

To evaluate the contact force, we use a compliant contact force model based on the Hertzian contact theory. In this contact force model, a body can be interpenetrated into the other body with a velocity. From this penetration information and geometrical configurations, compliant normal and friction forces are generated between the contact pair. In this compliant contact force model, the contact normal force can be defined as below:

$$f_n = k\delta^{m_1} + c \frac{\dot{\delta}}{|\dot{\delta}|} |\dot{\delta}|^{m_2} \delta^{m_3}, \tag{12}$$

where k and c are the spring and damping coefficients which are determined by an experimental way, respectively. $\dot{\delta}$ is a time differentiation of penetration δ . The exponents m_1 and m_2 generate a non-linear contact force, and the exponent m_3 yields an indentation damping effect. When the penetration velocity is very high when two bodies are separated after the maximum contact, the contact force can be negative due to a high negative damping force. But this situation is not realistic. This situation can be overcome by using an indentation damping exponent greater than one. The friction force is obtained by

$$f_f = \mu |f_n|, \tag{13}$$

where μ is the friction coefficient and its sign and magnitude can be determined from the relative velocity of the contact pair on the contact point.

3.3 Involute tooth profile

The gear teeth profile is usually defined as a special profile

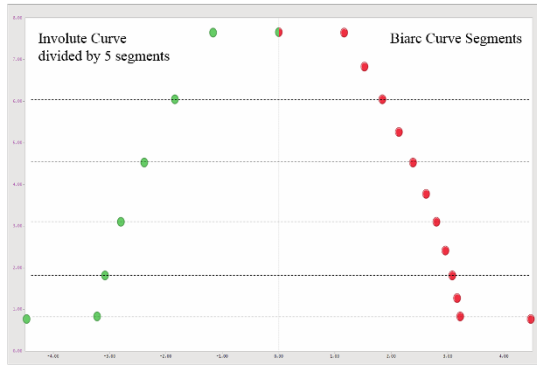


Fig. 5. Biarc curve fitting for the involute curve representation.

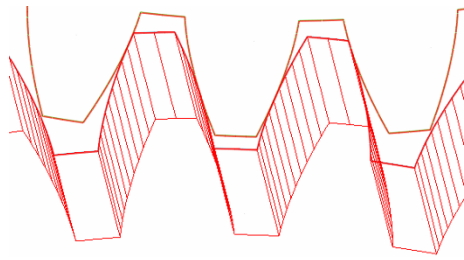


Fig. 6. Gear teeth contact.

called an involute curve because the contact line is maintained as a straight line. However, it is not efficient to use an extra involute profile in the contact search algorithm because of its complexity. To approximate the involute profiles, the biarc curve fitting method proposed by Bolton [7] is used in this investigation. The optimum biarc curve passing through a given set of points along the involute curve can be determined by this method. More arcs can be used to represent accurate involute profiles, but more calculation time will be consumed for searching the contacts.

Consequently, the real geometry of the involute tooth profiles consists of a series of arcs with the different radii as shown in Fig. 5.

3.4 Contact search algorithm

The contact algorithms for a gear pair are investigated in this study. The contact positions and penetration depth are defined from the kinematics of components. Thereafter, a concentrated contact force is generated at the contact point of the contact surface of the bodies. Efficient search algorithms should be considered seriously because there are large number of gear teeth, which can take a long time to search all teeth whether they are in contact or not.

For the efficient search of the gear-pinion contact kinematics, the contact search algorithm is divided into pre-search and post-search. In the pre-search, a bounding circle relative to the gear center is defined. All teeth of the pinion are employed to detect a starting and ending tooth, which has the possibility of contact with the gear teeth. Then, pinion teeth from starting

Table 2. Contact parameters.

Spring coefficient (Case1)	39.3×10^6 N/mm
Spring coefficient (Case2)	39.3×10^6 N/mm
Damping coefficient	1.0 N · s/mm
m_1	1.5
m_2	1.0
m_3	0.25

Table 3. Bending parameters.

Rotational spring coefficient	11.5×10^6 N · mm/rad
Rotational damping coefficient	0.2 N · mm · s/rad

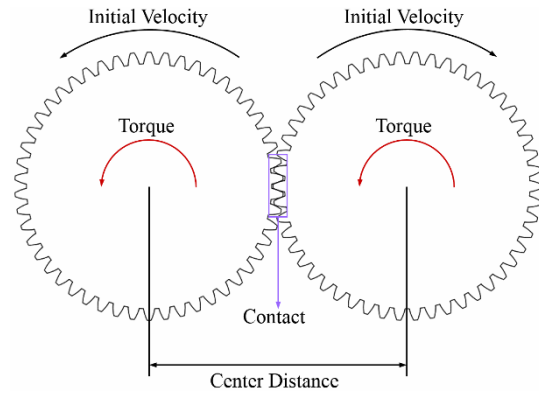


Fig. 7. Gear mesh model for DTE estimation.

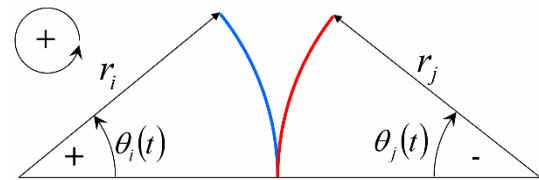


Fig. 8. Definition of dynamic transmission error (DTE).

tooth are investigated for the engagement with the gear teeth valley. The post-search means a detailed contact inspection between gear and pinion teeth with engagement. Once a starting and ending tooth is found at one time through the pre-search prior to the analysis, only a detailed search is carried out by using the information of engaged gear and pinion tooth from the next time step. There are two contact patterns such as arc-arc and arc-point contacts for the interaction between the gear and pinion tooth. The arc-arc and arc-point contact method which is proposed by Ryu [8, 9] is used in this investigation.

3.5 Contact and bending parameters

There are two major parameters for the quasi-flexible-body gear model: gear contact parameters and bending parameters between tooth and trunk.

For the bending parameters, the values can be obtained by

Table 4. Gear specification.

	Gear/pinion
Module	3 mm
Number of teeth	50
Pressure angle	20 degree
Radius of pitch circle	75 mm
Radius of outside circle	78 mm
Radius of base circle	70.477 mm
Radius of root circle	71.25 mm
Tooth width	20 mm
Elasticity modulus	$200 \times 10^9 \text{ N/m}^2$
Density	$7.85 \times 10^3 \text{ kg/m}^3$
Center distance	150 mm
Backlash	-0.002 mm

Table 5. Simulation condition.

Gear mesh frequency	700~3500 Hz
Preload torque	100, 200, 300 Nm

an experiment way or an FEM analysis in advance.

4. Validation method

The influence of a force response, involute contact ratio (ICR), and involute tip relief on the torsional vibration behavior of a spur gear is investigated experimentally by Kahraman and Blankenship [1, 10]. The torsional vibration behavior of a spur gear causes the noises. The prediction of the dynamic transmission error (DTE) is used as the estimator of the gear noise performance and dynamic tooth loading. The dynamic model may be reduced to a single DOF in terms of the DTE coordinate, which represents relative displacement across the gear mesh interface. DTE is defined as follows:

$$\text{DTE} = x(t) = r_i \theta_i(t) + r_j \theta_j(t), \quad (14)$$

where i and j are mesh gear pair, $\theta(t)$ is the rotational angle of each gear, and r is the base circle radius of each gear.

The mesh frequency is defined as below:

$$f_m = N\Omega / 60, \quad (15)$$

where f_m is the gear mesh frequency in Hz, N is the number of teeth of gear, and Ω is the rotational speed of the gear in rpm.

$$\Omega = 60f_m / N. \quad (16)$$

There are overlapped DTE in special mesh frequency. Two DTE cannot be obtained using a constant rotational speed method. By decreasing or increasing the speed gradually, they can be evaluated. This sweep calculation method is needed to

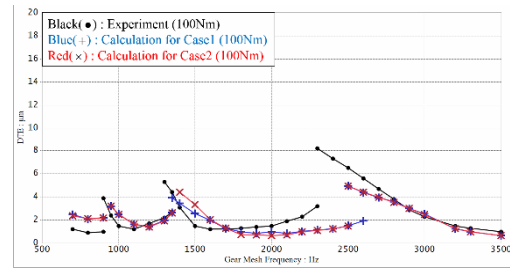


Fig. 9. Comparison between calculation and experiment (100 Nm).

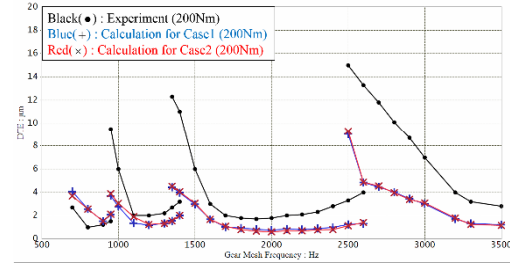


Fig. 10. Comparison between calculation and experiment (200 Nm).

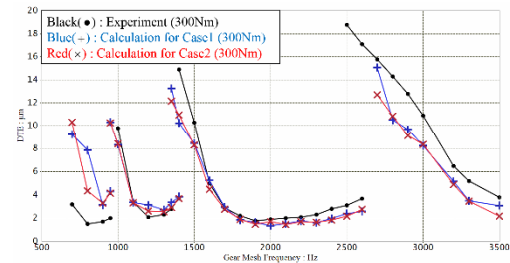


Fig. 11. Comparison between calculation and experiment (300 Nm).

get DTE in some mesh frequency range.

5. Result comparison

5.1 The test specification

The same gear specification is used for both gear and pinion. Simulation is performed for the preload torque 100, 200, and 300 Nm cases. Then, DTE is obtained by passing through 700~3500 mesh frequency for each torque cases.

5.2 Comparison between calculation and experiment

Simulation results of the root-mean-square (RMS) DTE are compared with an equivalent RMS amplitude obtained from the tree-term harmonic balance solution in Figs. 9-11 over the frequency range $700 \leq f_m \leq 3500$ Hz for each torque case (100, 200, 300 Nm). There are three lines in each figure: the black(•) line is the experimental data [1, 10], the blue(+) line is the Case1 results, and the red(x) line is the case 2 results.

As shown in Figs. 9-11, the results of cases 1 and 2 show a good agreement with the experimental data for the each torque case (100, 200, 300 Nm). But, the error of 200 Nm case is

Table 6. The ratio of simulation time for cases 1 and 2.

Preload torque	Case1	Case2
100 Nm	1.0	0.77
200 Nm	1.0	0.68
300 Nm	1.0	0.79

relatively larger than 100 and 300 Nm cases. The reason for the difference is not clear in the current research. The differences could be caused by the rigid assumption of gear tooth with simplified joint elements or numerical errors. As shown in the figures, the average of the error is around $3 \mu\text{m}$. The largest error is about $8 \mu\text{m}$ in 200 Nm case. This would be a sufficient accuracy for the application design. In addition, there is no big difference between the results of cases 1 and 2 models.

On the other hand, as shown in Table 6, regarding the calculation speed, case 2 is about twenty percent faster than case 1. There is no reference result to compare the calculation speed of case 1 because there are many simulation cases depending on the mesh frequency. Basically, case 1 model has 302 DOFs and case 2 has 102 DOFs in the QFB gear model. The simulation time varies mainly depending on the DOF and the complexity of the contact analysis. In general, the FEM model has much larger DOFs and contact search algorithm complexity than the proposed QFB gear model. These are the reasons why the all simulations with finite elements are very difficult. In this study, the gear DTE analysis could be performed with the proposed QFB gear models.

6. Conclusions

As mentioned, it is very important to grasp and reduce noise. The dynamic transmission error (DTE) is a good way to evaluate the whine noise, which is relatively related to high frequency characteristics. To estimate the DTE with a numerical method, Quasi-flexible-body gear modeling method has been used. This QFB gear modeling method was tested and developed in the commercial multi-body dynamics software RecurDyn [11].

The proposed QFB gear model has a rotational joint with a bending stiffness for joining the tooth and trunk for flexibility. This numerical model showed a good agreement with the experimental results. In addition, it was effective in the viewpoint of the calculation time and convenient for estimating the gear DTE.

Acknowledgment

This research was supported by the MOTIE (Ministry of Trade, Industry & Energy) and the KIAT(Korea Institute for Advancement of Technology) through the Industry Convergence/Connected for Creative Robot Human Resource Development (N0001126).

Nomenclature

\mathbf{r}	: Position vector of the body w.r.t. the global
$\boldsymbol{\omega}$: Angular velocity vector of the body w.r.t. the global
\mathbf{A}	: Orientation matrix of a body
\mathbf{Y}	: Cartesian local velocity vector
\mathbf{Z}	: Cartesian position vector
\mathbf{q}	: Relative generalized coordinates
f_n	: Contact normal force
f_f	: Contact friction force
μ	: Friction coefficient
k	: Spring coefficient of the contact
c	: Damping coefficient of the contact
m_1	: Stiffness exponent of the contact
m_2	: Damping exponent of the contact
m_3	: Indentation exponent of the contact
δ	: Penetration depth of the contact
$\dot{\delta}$: Time derivative of the penetration depth
f_m	: Gear mesh frequency

References

- [1] G. W. Blankenship and A. Kahraman, Gear dynamics experiments, Part-I : Characterization of forced response, *ASME, Power Transmission and Gearing Conference*, San Diego (1996).
- [2] J. G. Jalón and E. Bayo, *Kinematic and dynamic simulation of multibody systems*, Springer-Verlag, New-York (1994).
- [3] D. S. Bae, J. M. Han, J. H. Choi and S. M. Yang, A generalize recursive formulation for constrained flexible multibody dynamics, *International J. for Numerical Methods in Engineering*, 50 (2001) 1841-1859.
- [4] J. Choi, A study on the analysis of rigid and flexible body dynamics with contact, *Ph.D. Dissertation*, Seoul National University, Seoul (2009).
- [5] D. J. García de Jalón, J. Unda and A. Avello, Natural coordinates for the computer analysis of multibody systems, *Computer Methods in Applied Mechanics and Engineering*, 56 (1986) 309-327.
- [6] J. Wittenburg, *Dynamics of systems of rigid bodies*, BF Teubner, Stuttgart (1977).
- [7] K. M. Bolton, Biarc curves, *Computer Aided Design*, 7 (2) (1975) 89-92.
- [8] H. S. Ryu and K. C. Jang, Dynamic analysis of spur gear pairs : Mesh forces with efficient contact analysis, *ACMD* (2002).
- [9] D. Suzuki, S. Horiuchi, J. Choi and H. Ryu, Dynamic analysis of contacting spur gear pair for fast system simulation, *J. of Solid State Phenomena*, 110 (2006) 151-162.
- [10] G. W. Blankenship and A. Kahraman, Steady state force response of a mechanical oscillator with combined parametric excitation and clearance type non-linearity, *J. of Sound and Vibration*, 185 (1995) 743-765.
- [11] RecurDyn User Manual, <http://functionbay.co.kr> (2014).



Sunggyu Cho received his M.S. in Mechanical Engineering from Kyunghee University, South Korea in 2008. He is currently an associate research engineer at FunctionBay, Inc.



Jin Hwan Choi received his M.S. and Ph.D. in Mechanical Engineering from the University of Illinois at Chicago in 1992 and 1996, respectively. He is currently a Professor at Kyunghee University of Mechanical Engineering.



Juhwan Choi received his M.S. and Ph.D. in Mechanical and Aerospace Engineering from Seoul National University, South Korea in 2000 and 2009, respectively. He is currently a Chief Product Officer at FunctionBay, Inc.



Sungsoo Rhim received his B.S. and M.S. in Mechanical Engineering from Seoul National Univ., Korea, in 1990 and 1992, respectively, and his Ph.D. from Georgia Institute of Technology in 2000. He is currently an Associate Professor at Kyunghee University of Mechanical Engineering.